Environ Sci Pollut Res (2017) 24:19126–19137
DOI 10.1007/s11356-017-9584-2

RESEARCH ARTICLE

Impacts of hydrologic variations on chemical weathering and solute sources in the Min River basin, Himalayan–Tibetan region

Jun Zhong[1,2] · **Si-liang Li**[3,4] · **Faxiang Tao**[1] · **Hu Ding**[1] · **Jing Liu**[1,2]

Received: 18 November 2016 / Accepted: 19 June 2017 / Published online: 28 June 2017

Abstract Feedback between hydrologic variations and chemical weathering is thought to play a crucial role in modulating global carbon cycling. The mechanisms associated with the impacts of hydrologic variations on solute sources and chemical weathering were evaluated by examining the relationships between river discharge and hydrochemistry based on high-frequency sampling of the Min River, which originates in the Himalayan–Tibetan region. Fluid transit times and flow pathways vary with changes in discharge, thereby affecting various biogeochemical processes. Although shorter transit times occur during the high-flow season than during the low-flow season, concentrations of chemical weathering products exhibit chemostatic behaviour (less variation than changes in discharge) in response to increasing discharge due to hydrologic flushing of minerals, which increases the amount of reactive mineral surface area. The contributions of various sources to dissolved loads in the Min River were estimated using a forward model. The calculated annual carbonate and silicate weathering fluxes are 24.1 and 9.6 t/km^2 year, respectively. Atmospheric contributions increase with increasing discharge, whereas the contributions of silicate weathering decrease with increasing discharge. Both the carbonate weathering flux (F_{Carb}) and silicate weathering flux (F_{Sil}) are positively correlated with the discharge, indicating that temporal variations in chemical weathering fluxes in the Min River are highly affected by hydrologic variations. The slope of the relationship between F_{Carb} and discharge is much greater than that between F_{Sil} and discharge due to the rapid dissolution of carbonate minerals, suggesting that carbonate weathering is more sensitive than silicate weathering to hydrologic variations. This study demonstrates that high-frequency sampling is necessary when investigating solute sources and chemical weathering processes in river basins influenced by a monsoon climate.

Keywords Hydrologic variations · Fluid transit time · Chemical weathering · Chemostatic behaviour · Dissolution kinetics · Himalayan–Tibetan region

Responsible editor: Boqiang Qin

Electronic supplementary material The online version of this article (doi:10.1007/s11356-017-9584-2) contains supplementary material, which is available to authorized users.

✉ Si-liang Li
siliang.li@tju.edu.cn

[1] State Key Laboratory of Environmental Geochemistry, Institute of Geochemistry, Chinese Academy of Sciences, Guiyang 550081, China

[2] University of Chinese Academy of Sciences, Beijing 100049, China

[3] Institute of Surface-Earth System Science, Tianjin University, Tianjin 300072, China

[4] State Key laboratory of Hydraulic Engineering Simulation and Safety, Tianjin University, Tianjin 300072, China

Introduction

Rivers play a key role in transporting solutes produced by continental chemical weathering to the ocean (Edmond et al. 1995; Han and Liu 2004, Meybeck 1993, Natali et al. 2016). The removal of atmospheric CO_2 by chemical weathering is thought to provide feedback that regulates the climate on global and regional scales over geologic time (Berner and Caldeira 1997; Gao et al. 2009; Hren et al. 2007, White and Blum 1995). However, quantifying the effects of hydrologic variations on chemical weathering and its response to biogeochemical processes has proved to be difficult and controversial (Tipper et al. 2006). The concentrations of solutes in rivers depend on biogeochemical processes such as chemical weathering, precipitation, ion exchange and other reactions.

Hydrologic variations such as dilution by rain and mixing of "old" and "new" waters have large impacts on dissolved loads in rivers (Basu et al. 2010; Douglas 2006; Gabet et al. 2006; Gascuel-Odoux et al. 2010; Li et al. 2015). Meanwhile, solute transport and chemical weathering are sensitive to hydrologic variations in a river basin, which is commonly reflected in the relationship between solute concentrations and hydrologic conditions (Clow and Mast 2010; Godsey et al. 2009; Moon et al. 2014; Moquet et al. 2016; Torres et al. 2015). To investigate the relationships between hydrologic variations and chemical weathering, a temporal rather than spatial approach should be adopted (Clow and Mast 2010).

Temporal (e.g. seasonal) variations in major ion concentrations have been previously reported in rivers draining the Himalayan–Tibetan region (Chalk et al. 2015; Chapman et al. 2015; Galy and France-Lanord 1999; Singh et al. 2005; Tipper et al. 2006). Chalk et al. (2015) concluded that temporal variations in major ions were derived from variations in inputs from the various Himalayan lithotectonic units. Galy and France-Lanord (1999) attributed the chemical signal in their study to the dissolution of soil carbonate. Tipper et al. (2006) suggested that carbonate weathering is more sensitive than silicate weathering to monsoon runoff. Qin et al. (2006) focused on monthly variations in water chemistry and chemical weathering in the Min River. However, the sensitivity of chemical weathering to hydrologic variations and the relationship between chemical weathering fluxes and discharge have not been investigated well. Moon et al. (2014) suggested that at least 10 and preferably 40 temporally spaced samples with synchronous discharge are necessary to estimate chemical weathering rates accurately. However, few researchers have accurately explored high-frequency temporal variations in dissolved loads in rivers under various hydrologic conditions. Therefore, high-frequency sampling studies are needed to better understand weathering processes and their sensitivity to hydrologic variations.

This study involved the collection of samples at a high-frequency (monthly to daily sampling) from the Min River, which originates in the Himalayan–Tibetan region. Time series solute concentrations were used to investigate the relationships among element dynamics, element ratios, chemical weathering rates and hydrologic variations. These relationships were used to study how hydrologic variations affect biogeochemical processes and to increase the knowledge of the links between chemical weathering and hydrologic variations.

Materials and methods

The Min River originates on the eastern margin of the Qinghai–Tibetan Plateau and flows through the industrialized, heavily populated and agricultural Sichuan Basin and into the Changjiang River, which is the world's fourth largest in terms of discharge (Qin et al. 2006). It is 793 km long and drains an area measuring 133,500 km^2. The Sichuan Basin is a relatively undeformed part of the Yangtze Platform, and its surface is at an average elevation of 500 m (Yoon et al. 2008). The elevation of the Min River changes significantly in the alluvial plain (Fig. 1). The mean annual precipitation is 1200–1500 mm in the Sichuan Basin (Yoon et al. 2008), and the seasonal monsoon results in considerable precipitation during the summer and little precipitation during the winter in the basin.

The upper and middle portions of the Min River basin are underlain by two geologic terranes: the Bayan-Har fold belt and the Longmenshan fold belt (Qin et al. 2006; Yoon et al. 2008). The Bayan-Har fold belt is composed exclusively of Triassic marine flysch deposits that are 5–15 km thick. This terrane is composed primarily of sandstone, shale and slate and to a lesser extent of carbonate and volcanic rocks and minor sandstones and mudstones interbedded with coal seams. The Longmenshan fold belt consists of a tectonic nappe composed of Precambrian and Palaeozoic meta-igneous and meta-sedimentary rocks that include carbonaceous slate and phyllite interbedded with marble, carbonate interbedded with clastic rocks and minor carbonaceous shale, and coal-bearing sandstone and mudstone (Qin et al. 2006). The area southwest of Leshan is underlain by carbonate intercalated with gypsum and halite, sandstone, shale, granite and a prominent Permian basalt (Qin et al. 2006; Yoon et al. 2008). The remainder of the Min River basin is underlain by fluvial deposits, reddish sandstone and mudstone.

Twenty-seven river water samples were collected at the outlet of the Min River (Fig. 1) near the Gaochang hydrologic station, which is located approximately 28 km from the Changjiang River. The Gaochang hydrologic station is the gauging site for the entire Min River, and data from this station would be used to determine the overall status of the river. Monthly samples for chemical analysis were collected from November 2013 to October 2014, i.e. spanning an entire hydrologic year. Additional samples were collected during high-discharge periods from June to August 2014. Electrical conductivity (Ec), pH and temperature (T) were measured in the field. Alkalinity was determined with 0.02 μM hydrochloric acid. The water samples were filtered through cellulose-acetate filter paper prior to analysis. The anions (SO_4^{2-}, Cl^- and NO_3^-) were analysed via ion chromatography using a Diones ICS90 (with an error of 5%). After acidification to a pH of 2 using ultra-purified HNO_3, the concentrations of major cations (K^+, Na^+, Ca^{2+} and Mg^{2+}) and Si were determined via inductively coupled plasma-optical emission spectrometry (ICP-OES) (with an error of 3%). All these measurements were conducted at the State Key Laboratory of Environmental Geochemistry (Institute of Geochemistry, Chinese Academy of Sciences). Additionally, daily water discharge data were obtained online from the Ministry of Water Resources of China (http://www.hydroinfo.gov.cn/).

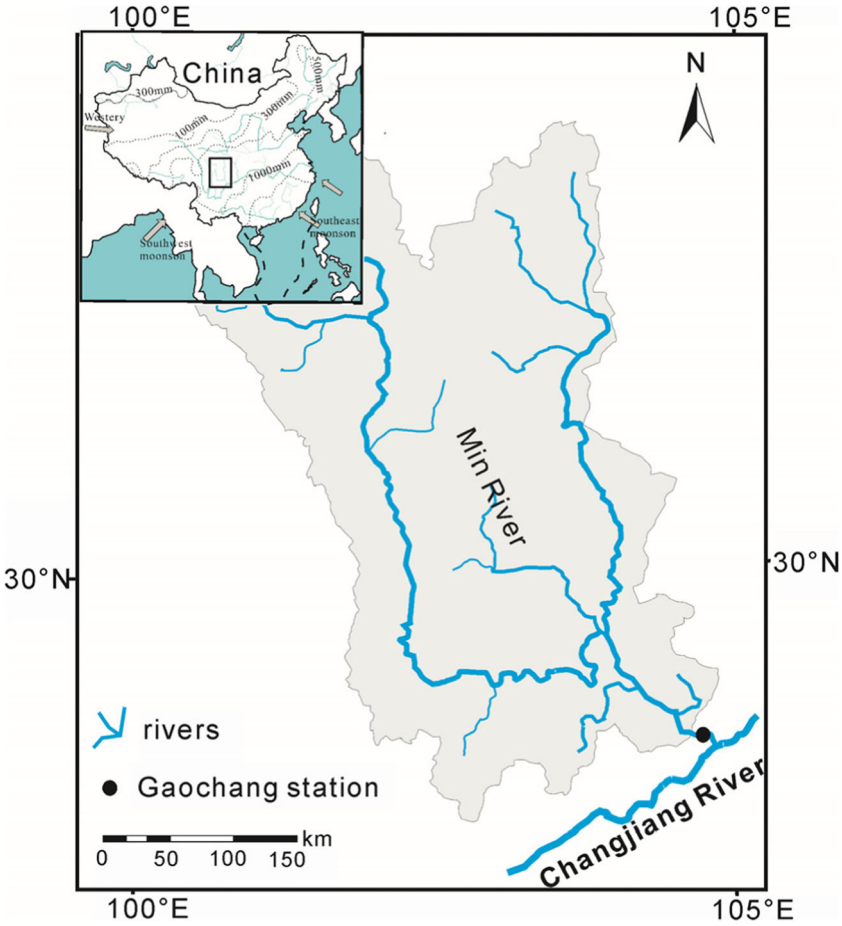

Fig. 1 Map showing the sampling site on the Min River

Results

The discharge and chemical characteristics of the Min River are presented in Table 1. The pH of the Min River (7.9 to 8.3) is mildly alkaline (Table 1). The Ec varies widely, from 222 to 344 μs/cm, with an average of 274.2 μs/cm. The total cation charge TZ^+ ($TZ^+ = 2Ca^{2+} + 2\ Mg^{2+} + Na^+ + K^+$) ranges from 2543 to 3959 μeq, and the total anion charge TZ^- ($TZ^- = HCO_3^- + 2SO_4^{2-} + Cl^- + NO_3^-$) is 2400–3633 μeq. The normalized inorganic charge balances ($NICB = (TZ^+ - TZ^-) \times 100\%/(TZ^+ + TZ^-)$) of the samples vary within ±5%. The mean flow-weighted concentration of total dissolved solids (TDS) is 219.8 mg/L, which is much higher than the world average of 97 mg/L (Li et al. 2014b). As in most Himalayan rivers (Table 2), the dissolved load is dominated by Ca^{2+} and HCO_3^-. The mean flow-weighted concentrations of the major cations rank as follows: $Ca^{2+} > Na^+ \approx Mg^{2+} > K^+$; this ranking is similar to those observed in the Mekong River (Li et al. 2014b) and Irrawaddy River (Chapman et al. 2015). The anion concentrations in the Min River rank as follows: $HCO_3^- > SO_4^{2-} > Cl^- > NO_3^-$. The ion compositions differ from those of rivers that are highly affected by evaporite dissolution with extremely high concentrations of Na^+ and Cl^-, such as the Jinsha River (Noh et al. 2009, Wu et al. 2008), the Lancang River (Wu et al. 2008), the Upper Yellow River (Wu et al. 2005, 2008) and the inland rivers draining the Himalayan–Tibetan region (Wu 2016). Higher levels of Cl^- were found in this study than in the monthly average data from 2005 reported by Qin et al. (2006).

Discussion

Element dynamics

Determining the temporal variations in dissolved loads allowed us to derive the relationships between the concentrations and discharge, which can be used to trace the sources of the solutes and analyse the associated biogeochemical processes. Power law functions (Eq. 1) have been used to model these relationships in several rivers (Clow and Mast 2010; Gislason et al. 2009; Godsey et al. 2009; Moon et al. 2014; Moquet et al. 2016; Torres et al. 2015):

$$C_i = a\ Q_i^b, \tag{1}$$

where C_i is the instantaneous concentration of major ions, a is a constant, Q_i is the daily discharge, and b is a regression

Table 1 Discharge and chemistry of the Min River

Parameter	Number of samples	Units	Max	Min	Average	S.D.	CV (%)	MFWC
Discharge	365	m^3/s	9560	715	2616	1876.61	71.74	
pH	27		8.3	7.9		0.15	1.88	8.2
Ec	27	μs/cm	344	222	274.2	35.03	12.77	260.9
Ca^{2+}	27	mg/L	44.6	33.6	38.4	2.98	7.75	37.5
Mg^{2+}	27	mg/L	12.9	6.1	8.4	1.76	20.89	7.7
Na^{+}	27	mg/L	15.6	4.1	8.3	3.13	37.53	7.0
K^{+}	27	mg/L	2.7	1.3	2.1	0.33	15.90	2.1
SiO_2	27	mg/L	7.5	5.8	6.7	0.56	8.30	6.8
HCO_3^-	27	mg/L	139.7	106.1	120.2	9.20	7.65	115.6
SO_4^{2-}	27	mg/L	46.8	22.5	30.7	6.06	19.74	29.0
Cl^-	27	mg/L	15.2	3.9	7.3	2.52	34.35	6.4
TDS	27	mg/L	282.2	198.2	229.9	23.87	10.38	219.8

S.D. standard deviation, *CV* coefficient of variation, *MFWC* mean flow-weighted concentration $(\sum(Q_iC_i)/\sum Q_i)$

coefficient describing the power dependence of solute concentration on river discharge. When b is zero, the concentration is independent of the discharge. This behaviour, called "chemostatic" behaviour (Godsey et al. 2009), reflects a solute concentration that remains constant with changes in discharge (Moquet et al. 2016). When b is equal to −1, the dissolved chemical concentrations are controlled by dilution with pure water (Gislason et al. 2009), reflecting a constant solute flux despite changing discharge (Moquet et al. 2016).

As shown in Fig. 2, the concentration–discharge plots of the solutes differ markedly, indicating that different biogeochemical processes affect the behaviours of the various elements. Ca^{2+}, Mg^{2+} and HCO_3^- are mainly derived from chemical weathering of carbonate, which involves relatively rapid dissolution kinetics. Moreover, calcite and dolomite precipitation modulate the concentrations of Ca^{2+}, Mg^{2+} and HCO_3^- when the saturation index (SI) is greater than 0. Therefore, Ca^{2+}, Mg^{2+} and HCO_3^- exhibit strongly stable biogeochemical behaviour in the Min River (Fig. 2), and their values of b in Eq. 1 exceed −0.3. The oxidation of sulphides is an important source of SO_4^{2-} in the rivers originating in the Qinghai–Tibetan Plateau (Galy and France-Lanord 1999; Karim and Veizer 2000; Li et al. 2014a), and river SO_4^{2-} is strongly affected by anthropogenic activities (Qin et al. 2006). The Na^+ and Cl^- concentrations in the Min River show significant dilution effects, with $b < -0.3$ (Fig. 2), indicating that evaporite dissolution is not the main source of major ions in the Min River. Potassium may be enriched in surface soil due to cation exchange and relatively high concentrations in biomass (Boy et al. 2008). No significant relationship exists between the K^+ concentrations and discharge of the Min River (Fig. 2), possibly due to the release of potassium from the soil. Eq. 1 for Si has a near-zero power law exponent, and the Si concentrations, which are controlled by various biogeochemical processes, vary little with changing discharge of the Min River (Fig. 2).

Metrics of chemostatic response

The ratio of the coefficients of variation (CV) of concentration and discharge (CV_C/CV_Q) has been proposed as an alternative, nonparametric measure of chemostatic response (Thompson et al. 2011):

$$\frac{CV_C}{CV_Q} = \frac{\mu_Q \sigma_C}{\mu_C \sigma_Q}, \quad (2)$$

where CV is the standard deviation σ of a variable normalized by its mean μ. Chemostatic behaviour occurs when the variation in concentration is highly buffered, i.e. $CV_C/CV_Q << 1$ (Thompson et al. 2011). When $CV_C/CV_Q = 1$, the solute concentrations are entirely controlled by the variations in discharge. Defining the condition of low CV_C/CV_Q values as chemostatic behaviour, however, should not be over interpreted (Thompson et al. 2011). Chemostatic behaviour does not mean that concentrations are not correlated with varying discharge or are entirely invariant. Instead, it indicates that the concentrations exhibit a low degree of variation in response to varying discharge.

Plots of the CV_C/CV_Q ratios of various elements in the Min River are shown in Fig. 3. Cl^- and Na^+ are conservative ions, and their concentrations show episodic behaviour (high CV_C/CV_Q ratios), as they do in other rivers originating in the Himalayan–Tibetan region (Fig. 3). Among these rivers, the Jinsha River displays the highest CV_C/CV_Q ratio, due to evaporite dissolution. The previous studies demonstrated that the oxidation of sulphides contributes large amounts of SO_4^{2-} to rivers originating in Himalayan–Tibetan region (Galy and France-Lanord 1999; Karim and Veizer 2000; Li et al. 2014a); therefore, SO_4^{2-} is associated with relatively high CV_C/CV_Q ratios. The K^+ in the Min River might be affected by cation exchange with the soil. Mg^{2+}, Ca^{2+} and HCO_3^- are

Table 2 Major ions and other chemical parameters of rivers draining the Himalayan–Tibetan region

River			pH	Ca^{2+} μmol/L	Mg^{2+} μmol/L	Na^{+} μmol/L	K^{+} μmol/L	HCO_3^{-} μmol/L	Cl^{-} μmol/L	SO_4^{2-} μmol/L	Si μmol/L	TDS mg/L	Source
Min River	Temporal	Mean	8.1	960	350	361	54	1970	206	320	112	230	This study
Min River	Spatial	Mean		727	321			1941	79	172	113	181	Chen et al. (2002)
Min River	Temporal	Mean	8.2	1234	413	234	24	2149	141	345	120	240	Qin et al. (2006)
Min River	Single	$N = 1$	7.8	916	343	496	66	1900	146	467	123	243	Chetelat et al. (2008)
Jinsha River	Spatial	Mean	7.9	931	495	3400	72	2066	2610	605	107	413	Noh et al. (2009)
Jinsha River	Single	$N = 1$		1168	590	1709	47	3847	998	334	135	411	Wu et al. (2008)
Dadu River	Temporal	Mean	8.5	960	395	98	16	2103	22	224	125	207	Qin et al. (2006)
Mekong River	Temporal &Spatial	Mean	7.6	836	347	336	52	1158	192	179	165	119	Li et al. (2014b)
Ganges River	Temporal	Mean	7.6	940	400	180	70	1420	90	160	130	130	Galy and France-Lanord (1999)
Brahmaputra River	Temporal	Mean	7.6	780	340	100	50	1110	20	120	160	110	Galy and France-Lanord (1999)
Ganges–Brahmaputra	Spatial	Mean		1420	992	613	69	2684	169	292	158	196	Sarin et al. (1989)
Indus River	Temporal	Mean	8.2	1274	420	191	68	1060	73	626	71	158	Karim and Veizer (2000)
Lancang River	Single	$N = 1$		1500	592	660	31	3696	415	452	142	381	Wu et al. (2008)
Nu River	Single	$N = 1$		1043	478	240	29	2761	33	281	238	263	Wu et al. (2008)
Upper Yellow River	Single	$N = 1$		1239	621	698	32	3697	313	236	109	347	Wu et al. (2008)
Yalong River	Single	$N = 1$		853	444	214	26	2518	29	146	124	222	Wu et al. (2008)
Upper Yellow River	Spatial	Mean	8.6	975	601	1260	46	2430	974	453	95	314	Wu et al. (2005)
Lanchang River	Spatial	Mean	8.1	769	271	323	26	1784	176	237	142	191	Noh et al. (2009)
Nu River	Spatial	Mean	7.7	621	364	220	29	1574	38	270	112	168	Noh et al. (2009)
Irrawaddy River	Spatial	Mean		370	234	276	33	1300	84	66	206	128	Chapman et al. (2015)
Salween River	Spatial	Mean		832	395	157	36	2288	34	163	146	211	Chapman et al. (2015)
Inland rivers	Spatial	Mean		1481	1172	1631	135	2910	1237	1443	120	607	Wu (2016)
World spatial median[a]	Spatial	Mean		1000	375	148	26	1256	96	219	134	127	Meybeck (2003)
World average[b]	Spatial	Discharge-weighted		594	245	240	44	798	167	175	145	97	Li et al. (2014b)

[a] Values were means calculated by adding data from the world's large rivers and dividing by the corresponding number of rivers

[b] Values were calculated by adding data from the world's large rivers, dividing by the corresponding number of rivers and weighting based on their discharges

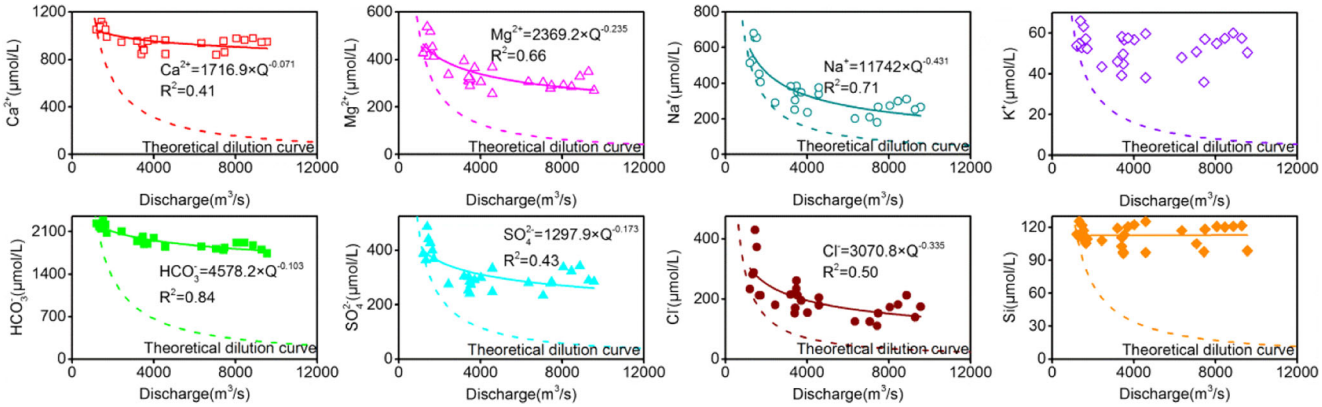

Fig. 2 Concentration–discharge relationships for solutes in the Min River

affected by both carbonate weathering and carbonate precipitation. Thus, these ions exhibit strongly chemostatic behaviour in response to the varying discharge. Many factors affect the Si content in the Min River, such as maintaining equilibrium with secondary silicate minerals (Torres et al. 2015) and retention of dissolved silica in reservoirs (Humborg et al. 1997). Therefore, Si exhibits strongly chemostatic behaviour in response to the varying discharge.

Identification of rock-weathering sources

As shown in Fig. 4a, the concentrations of Na^+ are higher than those of Cl^- in all the samples, indicating that silicate weathering is a non-negligible source, which is common among rivers originating in the Himalayan–Tibetan region. The concentrations of Na^+ and Cl^- are higher in the low-flow season than in the high-flow season, indicating significant dilution. The Na^+ and Cl^- concentrations are much lower than those of rivers greatly affected by evaporite dissolution, such as the Jinsha River (Wu et al. 2008) and the inland rivers (Wu 2016). A strong correlation between the Mg^{2+}/Na^+ and Ca^{2+}/Na^+ ratios is observed for the Min River, and significant differences exist between the low- and high-flow seasons (Fig. 4b). The Mg^{2+}/Na^+ and Ca^{2+}/Na^+ ratios in the Min River are higher during the high-flow season because of the faster dissolution of carbonate. The Mg^{2+}/Na^+ and Ca^{2+}/Na^+ ratios are close to their respective world discharge-weighted averages (Fig. 4b), and the chemistry of the Min River is controlled by carbonate and silicate weathering.

Relationships between element ratios and discharge

The relationships between the water chemistry and discharge, specifically, the coefficients of variation of concentration versus discharge presented in this study, were used to identify the ion sources and associated weathering processes. The element ratio–discharge relationships were used to understand the changes in solute contributions and to examine the related biogeochemical processes under various hydrologic conditions (Torres et al. 2015). The Na^*/Ca^{2+} ratio ($Na^* = Na^+ - Cl^-$) can be used to determine the relative contributions of silicate weathering versus carbonate weathering (Tipper et al. 2006; Torres et al. 2015). Furthermore, changes in the Si/Na* ratio are related to changes in differential dissolution/precipitation rates between minerals (Tipper et al. 2006) and represent the balance between secondary mineral precipitation and primary silicate weathering. The K^+/Na^* ratio was used to analyse the relative intensity of cation exchange in the soil. Finally, variations in the Cl^-/Na^* ratio represent the relative contributions of evaporite dissolution or anthropogenic activities versus silicate weathering (Torres et al. 2015).

Changes in the concentration–discharge relationships may be related to changes in the reaction time between water and minerals (Torres et al. 2015). Consequently, the water has less time to react with minerals during the high-flow season (Maher 2011; Maher and Chamberlain 2014; Torres et al. 2015). Therefore, most of the solute concentrations are affected by dilution with increasing discharge (Fig. 2). Element ratios are a particularly useful tool for investigating the biogeochemical processes acting in river basins (Torres et al. 2015). By investigating the variations in element ratios with respect to discharge, hydrologically driven changes in flow

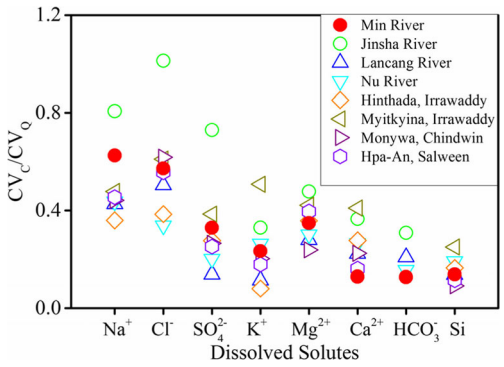

Fig. 3 Coefficients of variation of concentration versus discharge. The data regarding the Jinsha, Lancang and Nu Rivers are from (Huang 2015). The data regarding the streams near Hinthada, Myitkyina, Monywa and Hpa-An are from Chapman et al. (2015)

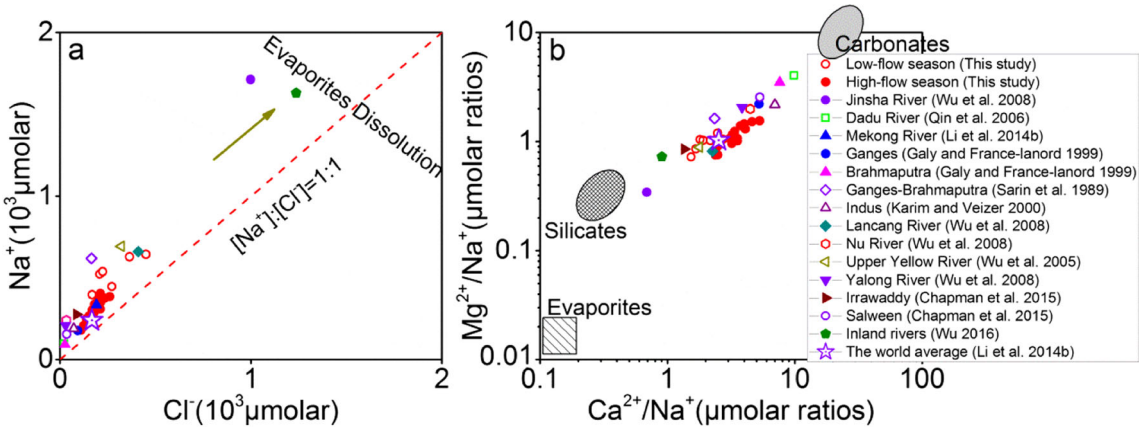

Fig. 4 **a** Variations in Cl^- and Na^+. **b** Molar ratios of Mg^{2+}/Na^+ versus Ca^{2+}/Na^+ in the Min River. The end-member compositions for carbonates, silicates and evaporites are from Gaillardet et al. (1999). We define November to May as the low-flow season and June to October as the high-flow season of the Min River

paths and biogeochemical processes can be identified (Calmels et al. 2011; Tipper et al. 2006; Torres et al. 2015). Because of the fast dissolution kinetics of carbonate weathering (Tipper et al. 2006; Zhong et al. 2017), the Na^*/Ca^{2+} ratios in the Min River tend to decrease with increasing river discharge (Fig. 5a). Increasing discharge decreases the transit time of fluids, leading to short times for the fluids and minerals to reach equilibrium with secondary Si-bearing phases (Maher 2011; Maher and Chamberlain 2014), short retention times in reservoirs in the upper river reaches (Humborg et al. 1997) and great release of biologic silica. Therefore, the Si/Na* ratio increases with increasing discharge of the Min River (Fig. 5b). Potassium being an exchangeable cation, soil layers can become enriched in potassium (Boy et al. 2008; Torres et al. 2015). With short transit times, there is insufficient time for the water to reach equilibrium with the soil. Thus, the K^+/Na^* ratio increases with increasing discharge (Fig. 5c). The Cl^- concentrations in the Min River are highly affected by anthropogenic activities (Qin et al. 2006), and the Cl^- concentrations in our samples are much higher than those reported by Qin et al. (2006) (Table 2). In the Min River, the Cl^-/Na^* ratio, which can be used to estimate the relative contributions of anthropogenic inputs and evaporite dissolution versus silicate weathering, increases with increasing river discharge (Fig. 5d). Therefore, the anthropogenic and evaporate-dissolution contributions exceed the silicate weathering contribution with increasing discharge.

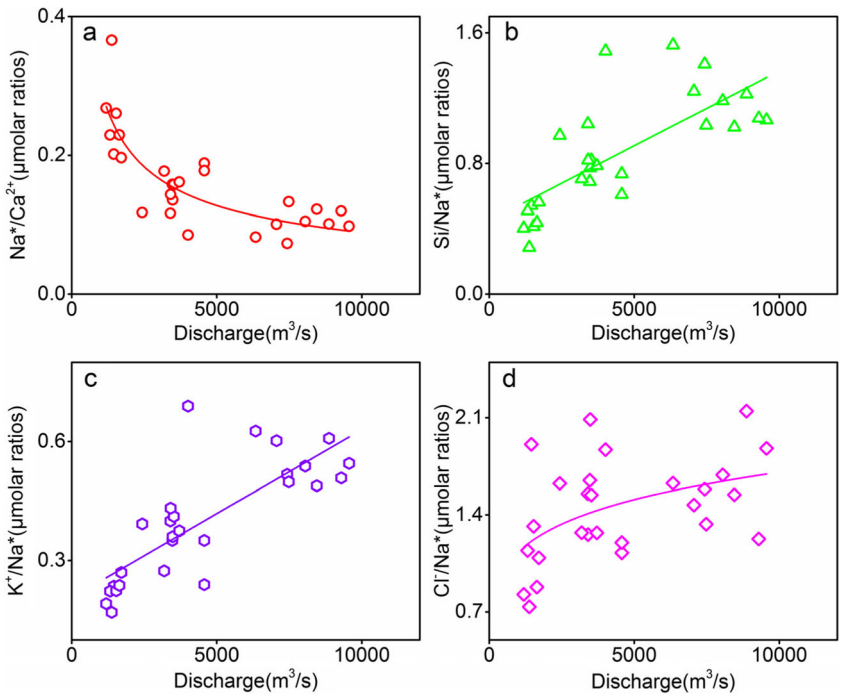

Fig. 5 Correlations between discharge and the Na^*/Ca^{2+} ratio, Si/Na* ratio, K^+/Na^* ratio and Cl^-/Na^* ratio in the Min River

Sources of major ions

The chemical composition of river water is generally controlled by atmospheric inputs, carbonate and silicate weathering, evaporite dissolution and anthropogenic inputs (Moon et al. 2007; Li et al. 2014b; Wang et al. 2016; Xiao et al. 2016). The budget equation for major ion X can be written as follows (Galy and France-Lanord 1999):

$$[X]_{riv} = [X]_{atm} + [X]_{carb} + [X]_{sil} + [X]_{eva} + [X]_{anth}, \quad (3)$$

where "riv" denotes river water; "atm" denotes atmospheric input; "carb", "sil" and "eva" denote the contributions of carbonate, silicate and evaporite dissolution, respectively; and "anth" denotes anthropogenic sources. Hot springs potentially control the water chemistry of rivers in the Himalayan–Tibetan region (Hren et al. 2007; Li et al. 2014a). Li et al. (2014a) suggested that hot springs contribute less than 3% of the dissolved loads in the Yalong River on the eastern Qinghai–Tibetan Plateau near the Min River. In this study, the contributions of other sources may be overestimated (Hren et al. 2007; Li et al. 2014a) after ignoring hot spring sources.

Atmospheric inputs

Atmospheric inputs are regarded as a non-negligible contributor to water chemistry (Wang et al. 2016; Xiao et al. 2015), although this contribution is very small in rivers draining the Himalayan–Tibetan region (Noh et al. 2009; Wu et al. 2008). The lowest Cl^- concentration in the basin (7 μmol/L; Qin et al. 2006) is assumed to be derived completely from atmospheric inputs, which is agreement with other previous studies (Han and Liu 2004; Li et al. 2014a). Therefore,

$$X_{atm} = (X/Cl)_{rain} \times [Cl^-]_{ref}, \quad (4)$$

where $(X/Cl)_{rain}$ is the ratio of measured ions to Cl^- in rainwater based on the data of Noh et al. (2009). $[Cl^-]_{ref}$ is the lowest Cl^- concentration in the basin.

Silicate weathering

Silicate weathering contributes Na^+ and K^+ from aluminosilicate weathering and Ca^{2+} and Mg^{2+} from calcium–magnesium silicate weathering to the river (Wang et al. 2016). In this study, we assumed that after performing atmospheric correction, the remaining K^+ is from silicate weathering. Using Cl_{riv} as an index of atmospheric inputs, evaporite dissolution and anthropogenic inputs, the silicate component of Na^+ was estimated as follows:

$$[Na^+]_{sil} = [Na^+]_{riv} - [Cl^-]_{riv} \quad (5)$$

$[Ca^{2+}]_{Sil}$ and $[Mg^{2+}]_{Sil}$ were calculated from $[Na^+]_{Sil}$ based on appropriate $(Ca^{2+}/Na^+)_{Sil}$ and $(Mg^{2+}/Na^+)_{Sil}$ ratios. Working on a global scale, Gaillardet et al. (1999) assigned values of $(Ca^{2+}/Na^+)_{Sil} = 0.35 \pm 0.15$ and $(Mg^{2+}/Na^+)_{Sil} = 0.24 \pm 0.12$ to small streams draining silicate rocks. Moon et al. (2007) assigned a similar value of $(Ca^{2+}/Na^+)_{Sil} = \sim 0.46$ to the Hong River, which drains the eastern Himalaya. In this study, a Ca^{2+}/Na^+ ratio of 0.35 and an Mg^{2+}/Na^+ ratio of 0.24 were assigned to the silicate weathering end-member source, similar to studies of the Three Rivers region of eastern Tibet (Noh et al. 2009).

Carbonate weathering

Carbonate weathering supplies mainly Ca^{2+} and Mg^{2+} to the Min River. In this study, we assumed that the Mg^{2+} remaining after atmospheric and silicate corrections is derived from carbonate weathering (Eq. 6). A Ca^{2+}/Mg^{2+} ratio of 2.5 was assigned to the carbonate weathering end-member source based on discussions presented by Chetelat et al. (2008), Li et al. (2014a) and Millot et al. (2003).

$$[Mg^{2+}]_{carb} = [Mg^{2+}]_{riv} - [Mg^{2+}]_{atm} - [Mg^{2+}]_{sil} \quad (6)$$

Evaporite dissolution and anthropogenic inputs

Qin et al. (2006) reported that chlorine water treatment, acid rain and Ca-rich sewage are potential pollution sources and estimated that evaporite dissolution accounts for 15% of the total cations after correcting for the anthropogenic inputs using a forward model. Neither of these sources, i.e. anthropogenic inputs and evaporite dissolution, can be neglected. However, it is difficult to distinguish the relative contributions of evaporite dissolution and anthropogenic inputs to the river. In this study, we treated evaporite dissolution and anthropogenic inputs as a single end-member contribution. The contribution of evaporite dissolution and anthropogenic inputs may be underestimated due to possible Ca^{2+} precipitation in the riverine system.

The results indicate that atmospheric inputs account for approximately 3.8% of the total river cations (Fig. 6). The atmospheric contributions increase with increasing discharge, indicating the effects of dilution. The percentage contributions of silicate weathering tend to decrease with increasing discharge (Fig. 6) because of the relatively slow reaction rates of silicate minerals. The percentage contributions of carbonate weathering vary broadly, from 50.7 to 69.9% (Fig. 6), and carbonate weathering dominates the chemistry of the Min River. However, the trend with increasing discharge is not clear. The contributions of anthropogenic inputs and evaporite dissolution may be underestimated because of calcite precipitation. Generally, the anthropogenic–evaporite contribution

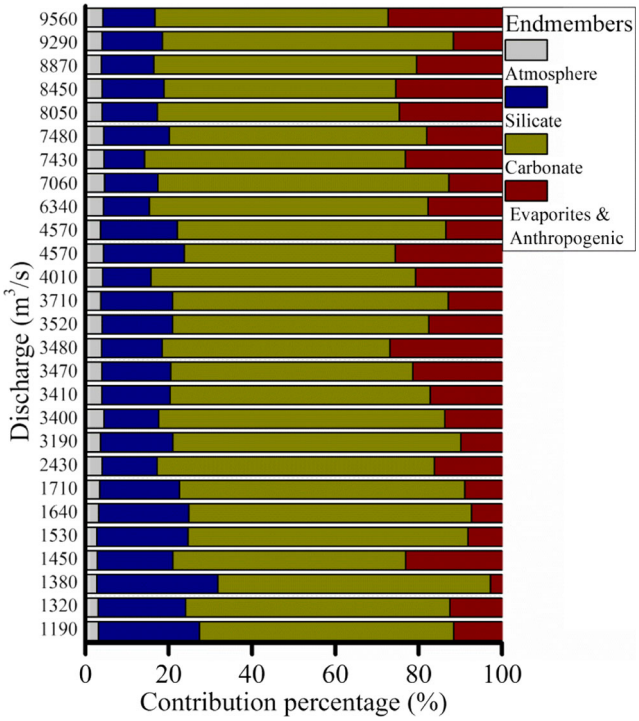

Fig. 6 Diagram showing contribution from different reservoirs in the Min River under various discharge conditions. The values on the *Y* axis are the instantaneous discharges at the instantaneous sampling times

under high-discharge conditions is much greater than that under low discharge conditions.

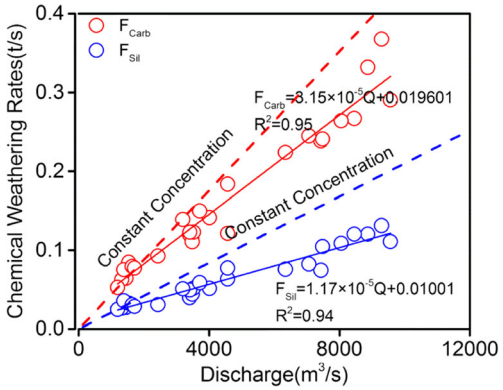

Fig. 7 Relationships between chemical weathering flux and discharge of the Min River

Fluxes due to carbonate and silicate weathering

The major-element dynamics are dominated by discharge changes (Fig. 2), and hydrologic flushing further induces chemostatic behaviour by increasing the amount of reactive mineral surface area, which accelerates mineral weathering (Clow and Mast 2010). The carbonate weathering flux (F_{Carb}) and silicate weathering flux (F_{Sil}) were calculated as follows:

$$F_{Carb} = \left(\left[Ca^{2+}\right]_{Carb} \times M_{Ca} + \left[Mg^{2+}\right]_{Carb} \times M_{Mg} \right) \times Discharge \quad (7)$$

$$F_{Sil} = \left(\left[Ca^{2+}\right]_{Sil} \times M_{Ca} + \left[Mg^{2+}\right]_{Sil} \times M_{Mg} + \left[Na^{+}\right]_{Sil} \times M_{Na} + \left[K^{+}\right]_{Sil} \times M_{K} + [Si] \times M_{SiO2} \right) \times Discharge, \quad (8)$$

where M is the molar mass of an element.

Based on these equations, F_{Carb} ranges from 52.6×10^{-3} to 367.5×10^{-3} t/s, with an average of 162.4×10^{-3} t/s. F_{Sil} ranges from 24.7×10^{-3} to 131.2×10^{-3} t/s, with a mean of 62.9×10^{-3} t/s. The values of F_{Carb} are much higher than those of F_{Sil} (Fig. 7.) because of the faster dissolution kinetics of carbonate. Although the transit time is shorter during the high-flow season, hydrologic flushing of minerals induces chemostatic behaviour by increasing the amount of reactive mineral surface area. These surface areas vary temporally in response to hydrologic variations (Clow and Mast 2010). Soil moisture with low discharge in the unsaturated zone may decrease to the point that the total mineral surface area becomes essentially unreactive. High discharge increases the soil moisture and the reactive mineral surface area. Therefore, although a shorter transit time causes greater dilution, increases in reactive mineral surface area will lead to chemostatic behaviour. Both F_{Carb} and F_{Sil} display positive relationships with discharge (Fig. 7), indicating that temporal variations in chemical weathering fluxes are highly affected by hydrologic variations. However, the plots of chemical weathering fluxes versus discharge are much lower than the line of constant concentration, suggesting that high-frequency sampling is necessary for accurately understanding the chemical weathering fluxes and biogeochemical processes. The slope of the F_{Carb} versus discharge plot is much higher than that of the F_{sil} versus discharge plot (Fig. 7) because carbonate dissolution is more sensitive than silicate dissolution to monsoonal runoff (Tipper et al. 2006; Zhong et al. 2017). Dissolution of rapidly weathering carbonate minerals might respond to the difference between F_{Carb} and F_{sil} under the various hydrological conditions.

The annual carbonate weathering flux (ACWF) and annual silicate weathering flux (ASWF) in the Min River were calculated using the following equations:

$$F_{Carb} = 3.15 \times 10^{-5} Q + 0.0196 \quad (9)$$

Table 3 Calculated values of ACWF and ASWF

ACWF (t/km^2 year)	ASWF (t/km^2 year)	Method
24.1	9.6	Our method[a]
30.0	12.5	Data from low-flow season[b]
21.7	8.3	Data from high-flow season[c]

[a] Results obtained from the use of Eqs. 11 and 12

[b] Chemical weathering flux based on sampling during the low-flow season (Nov 2013 to May 2014) and on the total annual discharge

[c] Chemical weathering flux based on sampling during the high-flow season (Jun 2014 to Oct 2014) and on the total annual discharge

$$F_{Sil} = 1.17 \times 10^{-5} Q + 0.0100 \quad (10)$$

$$ACWF = \sum_{n=1}^{365} (F_{Carb} \times 86400)/drainage\ area \quad (11)$$

$$ASWF = \sum_{n=1}^{365} (F_{Sil} \times 86400)/drainage\ area \quad (12)$$

The calculated ACWF is 24.1 t/km^2 year, and the ASWF is 9.6 t/km^2 year (Table 3). The ACWF and ASWF calculated using the data from only the low-flow season are 30.0 and 12.5 t/km^2 year, respectively (Table 3). Alternately, the ACWF and ASWF based on the data from the high-flow season are 21.7 and 8.3 t/km^2 year, respectively (Table 3). The annual chemical weathering fluxes are overestimated based on the data solely from the low-flow season and underestimated based on the data solely from the high-flow season. Therefore, high-frequency sampling is necessary for assessing the annual chemical weathering fluxes in monsoonal rivers.

Conclusions

This study investigated chemical weathering and solute sources impacted by hydrologic variations in the Min River of the Himalayan–Tibetan region based on time series sampling. The TDS concentrations in the Min River are much higher than the world average, are similar to those in other rivers in the Himalayan–Tibetan region and are lower than those in rivers greatly affected by evaporite dissolution. The solute concentrations in the Min River exhibit significant temporal variations. Most of these concentrations are lower during the high-flow season because of dilution. Power law functions in the concentration–discharge and CV_C/CV_Q relationships suggest that the element characteristics and solute sources control the variations in solute concentrations with changing discharge and that, although the solute concentrations vary significantly with time, these ions exhibit various level of chemostatic behaviour in response to hydrologic variations. The variations in element ratio–discharge relationships suggest that fluid transit times and flow pathways change with varying discharge, causing changes in various biogeochemical processes that affect the chemistry of the Min River. Based on the forward model, carbonate weathering dominates the river chemistry in this basin. The contributions of atmospheric inputs increase with increasing discharge, whereas the contributions of silicate weathering decrease with increasing discharge. The contributions of carbonate weathering and anthropogenic–evaporite sources do not exhibit clear trends with increasing discharge. F_{Carb} ranges from 52.6×10^{-3} to 367.5×10^{-3} t/s, with an average of 162.4×10^{-3} t/s, and F_{Sil} ranges from 24.7×10^{-3} to 131.2×10^{-3} t/s, with a mean of 62.9×10^{-3} t/s. Both F_{Carb} and F_{Sil} display positive relationships with discharge, indicating that temporal variations in chemical weathering are highly affected by hydrologic variations. Because of the faster dissolution kinetics of carbonate, the slope of the F_{Carb} versus discharge plot is much greater than that of the F_{sil} versus discharge plot. These findings suggest that high-frequency sampling is necessary to accurately assess the correlations among chemical weathering fluxes, biogeochemical processes and hydrologic variations in a river system. The significant relationships between chemical weathering fluxes and discharge of the Min River are presented, and these relationships can help in predicting the chemical weathering fluxes based on the discharge. Chemical weathering fluxes and solute dynamics in the Min River basin are highly sensitive to the hydrologic variations. The chemical weathering will respond rapidly to hydrologic variations, and such rapid changes may lead to global and regional carbon imbalances.

Acknowledgements This work was financially supported by National Natural Science Foundation of China (Grants 41422303 and 41130536) and the Ministry of Science and Technology of China (Grants 2016YFA0601000 and 2013CB956700).

References

Basu NB, Destouni G, Jawitz JW, Thompson SE, Loukinova NV, Darracq A, Zanardo S, Yaeger M, Sivapalan M, Rinaldo A, Rao PSC (2010) Nutrient loads exported from managed catchments reveal emergent biogeochemical stationarity. Geophys Res Lett 37: L23404. doi:10.1029/2010GL045168

Berner RA, Caldeira K (1997) The need for mass balance and feedback in the geochemical carbon cycle. Geology 25:955. doi:10.1130/0091-7613(1997)025<0955:TNFMBA>2.3.CO;2

Boy J, Valarezo C, Wilcke W (2008) Water flow paths in soil control element exports in an Andean tropical montane forest. Eur J Soil Sci 59:1209–1227. doi:10.1111/j.1365-2389.2008.01063.x

Calmels D, Galy A, Hovius N, Bickle M, West AJ, Chen M-C, Chapman H (2011) Contribution of deep groundwater to the weathering budget in a rapidly eroding mountain belt, Taiwan. Earth Planet Science Lett 303:48–58. doi:10.1016/j.epsl.2010.12.032

Chalk PM, Inácio CT, Urquiaga S, Chen D (2015) 13C isotopic fractionation during biodegradation of agricultural wastes. Isot Environ Health Stud 51:201–213. doi:10.1080/10256016.2015.1019488

Chapman H, Bickle M, Thaw SH, Thiam HN (2015) Chemical fluxes from time series sampling of the Irrawaddy and Salween Rivers, Myanmar. Chem Geol 401:15–27. doi:10.1016/j.chemgeo.2015.02.012

Chen J, Wang F, Xia X, Zhang L (2002) Major element chemistry of the Changjiang (Yangtze River). Chem Geol 187:231–255. doi:10.1016/S0009-2541(02)00032-3

Chetelat B, Liu C-Q, Zhao ZQ, Wang QL, Li SL, Li J, Wang BL (2008) Geochemistry of the dissolved load of the Changjiang Basin rivers: anthropogenic impacts and chemical weathering. Geochim Cosmochim Acta 72:4254–4277. doi:10.1016/j.gca.2008.06.013

Clow DW, Mast MA (2010) Mechanisms for chemostatic behavior in catchments: implications for CO2 consumption by mineral weathering. Chem Geol 269:40–51. doi:10.1016/j.chemgeo.2009.09.014

Douglas TA (2006) Seasonality of bedrock weathering chemistry and CO2 consumption in a small watershed, the White River, Vermont. Chem Geol 231:236–251. doi:10.1016/j.chemgeo.2006.01.024

Edmond JM, Palmer MR, Measures CI, Grant B, Stallard RF (1995) The fluvial geochemistry and denudation rate of the Guayana Shield in Venezuela, Colombia, and Brazil. Geochim Cosmochim Acta 59:3301–3325. doi:10.1016/0016-7037(95)00128-M

Gabet EJ, Edelman R, Langner H (2006) Hydrological controls on chemical weathering rates at the soil-bedrock interface. Geology 34:1065. doi:10.1130/G23085A.1

Gaillardet J, Dupré B, Louvat P, Allègre CJ (1999) Global silicate weathering and CO2 consumption rates deduced from the chemistry of large rivers. Chem Geol 159:3–30. doi:10.1016/S0009-2541(99)00031-5

Galy A, France-Lanord C (1999) Weathering processes in the Ganges–Brahmaputra basin and the riverine alkalinity budget. Chem Geol 159:31–60. doi:10.1016/S0009-2541(99)00033-9

Gao Q, Tao Z, Huang X, Nan L, Yu K, Wang Z (2009) Chemical weathering and CO2 consumption in the Xijiang River basin, South China. Geomorphology 106:324–332. doi:10.1016/j.geomorph.2008.11.010

Gascuel-Odoux C, Aurousseau P, Durand P, Ruiz L, Molenat J (2010) The role of climate on inter-annual variation in stream nitrate fluxes and concentrations. Sci Total Environ 408:5657–5666. doi:10.1016/j.scitotenv.2009.05.003

Gislason SR, Oelkers EH, Eiriksdottir ES, Kardjilov MI, Gisladottir G, Sigfusson B, Snorrason A, Elefsen S, Hardardottir J, Torssander P, Oskarsson N (2009) Direct evidence of the feedback between climate and weathering. Earth Planet Science Lett 277:213–222. doi:10.1016/j.epsl.2008.10.018

Godsey SE, Kirchner JW, Clow DW (2009) Concentration-discharge relationships reflect chemostatic characteristics of US catchments. Hydrol Process 23:1844–1864. doi:10.1002/hyp.7315

Han G, Liu C-Q (2004) Water geochemistry controlled by carbonate dissolution: a study of the river waters draining karst-dominated terrain, Guizhou Province, China. Chem Geol 204:1–21. doi:10.1016/j.chemgeo.2003.09.009

Hren MT, Chamberlain CP, Hilley GE, Blisniuk PM, Bookhagen B (2007) Major ion chemistry of the Yarlung Tsangpo–Brahmaputra River: chemical weathering, erosion, and CO2 consumption in the southern Tibetan Plateau and eastern syntaxis of the Himalaya. Geochim Cosmochim Acta 71:2907–2935. doi:10.1016/j.gca.2007.03.021

Huang L (2015) Chemical weathering in the Three Rivers region of southwestern China. University of Chinese Academy of Sciences, Master Thesis

Humborg C, Ittekkot V, Cociasu A, Bodungen VB (1997) Effect of Danube River dam on Black Sea biogeochemistry and ecosystem structure. Nature 386:385–388

Karim A, Veizer J (2000) Weathering processes in the Indus River Basin: implications from riverine carbon, sulfur, oxygen, and strontium isotopes. Chem Geol 170:153–177. doi:10.1016/S0009-2541(99)00246-6

Li S, Chetelat B, Yue F, Zhao Z, Liu C-Q (2014a) Chemical weathering processes in the Yalong River draining the eastern Tibetan Plateau, China. J Asian Earth Sci 88:74–84. doi:10.1016/j.jseaes.2014.03.011

Li S, Lu XX, Bush RT (2014b) Chemical weathering and CO_2 consumption in the Lower Mekong River. Sci Total Environ 472:162–177. doi:10.1016/j.scitotenv.2013.11.027

Li X, Gan Y, Zhou A, Liu Y (2015) Relationship between water discharge and sulfate sources of the Yangtze River inferred from seasonal variations of sulfur and oxygen isotopic compositions. J Geochem Explor 153:30–39. doi:10.1016/j.gexplo.2015.02.009

Maher K (2011) The role of fluid residence time and topographic scales in determining chemical fluxes from landscapes. Earth Planet Science Lett 312:48–58. doi:10.1016/j.epsl.2011.09.040

Maher K, Chamberlain CP (2014) Hydrologic regulation of chemical weathering and the geologic carbon cycle. Science 343:1502–1504. doi:10.1126/science.1250770

Meybeck M (1993) Riverine transport of atmospheric carbon: sources, global typology and budget. Water Air Soil Pollut 70:443–463. doi:10.1007/BF01105015

Meybeck M (2003) 5.08 - Global occurrence of major elements in rivers A2 - Holland, Heinrich D. In: Turekian KK (ed) Treatise on geochemistry. Pergamon, Oxford, pp 207–223

Millot R, Jé G, Dupré B, Allègre CJ (2003) Northern latitude chemical weathering rates: clues from the Mackenzie River Basin, Canada. Geochim Cosmochim Acta 67:1305–1329. doi:10.1016/S0016-7037(02)01207-3

Moon S, Chamberlain CP, Hilley GE (2014) New estimates of silicate weathering rates and their uncertainties in global rivers. Geochim Cosmochim Acta 134:257–274. doi:10.1016/j.gca.2014.02.033

Moon S, Huh Y, Qin J, van Pho N (2007) Chemical weathering in the Hong (Red) River basin: rates of silicate weathering and their controlling factors. Geochim Cosmochim Acta 71:1411–1430. doi:10.1016/j.gca.2006.12.004

Moquet JS, Guyot JL, Crave A, Viers J, Filizola N, Martinez JM, Oliveira TC, Sánchez LS, Lagane C, Casimiro WS, Noriega L, Pombosa R (2016) Amazon River dissolved load: temporal dynamics and annual budget from the Andes to the ocean. Environ Sci Pollut Res Int 23:11405–11429. doi:10.1007/s11356-015-5503-6

Natali C, Bianchini G, Marchina C, Knöller K (2016) Geochemistry of the Adige River water from the Eastern Alps to the Adriatic Sea (Italy): evidences for distinct hydrological components and water-rock interactions. Environ Sci Pollut Res Int 23:11677–11694. doi:10.1007/s11356-016-6356-3

Noh H, Huh Y, Qin J, Ellis A (2009) Chemical weathering in the Three Rivers region of Eastern Tibet. Geochim Cosmochim Acta 73:1857–1877. doi:10.1016/j.gca.2009.01.005

Qin J, Huh Y, Edmond JM, Du G, Ran J (2006) Chemical and physical weathering in the Min Jiang, a headwater tributary of the Yangtze River. Chem Geol 227:53–69. doi:10.1016/j.chemgeo.2005.09.011

Sarin MM, Krishnaswamy S, Dilli K, Somayajulu BLK, Moore WS (1989) Major ion chemistry of Ganga–Brahmaputra river system: weathering processes and fluxes of the Bay of Bengal. Geochim Cosmochim Acta 53:997–1009

Singh SK, Sarin MM, France-Lanord C (2005) Chemical erosion in the eastern Himalaya: major ion composition of the Brahmaputra and δ13C of dissolved inorganic carbon. Geochim Cosmochim Acta 69:3573–3588. doi:10.1016/j.gca.2005.02.033

Thompson SE, Basu NB, Lascurain J, Aubeneau A, Rao PSC (2011) Relative dominance of hydrologic versus biogeochemical factors on solute export across impact gradients. Water Resour Res 47:WOOJ05. doi: 10.1029/2010WR009605

Tipper ET, Bickle MJ, Galy A, West AJ, Pomiès C, Chapman HJ (2006) The short term climatic sensitivity of carbonate and silicate weathering fluxes: insight from seasonal variations in river chemistry. Geochim Cosmochim Acta 70:2737–2754. doi:10.1016/j.gca.2006.03.005

Torres MA, West AJ, Clark KE (2015) Geomorphic regime modulates hydrologic control of chemical weathering in the Andes–Amazon. Geochim Cosmochim Acta 166:105–128. doi:10.1016/j.gca.2015.06.007

Wang L, Zhang L, Cai W-J, Wang B, Yu Z (2016) Consumption of atmospheric CO2 via chemical weathering in the Yellow River basin: the Qinghai–Tibet Plateau is the main contributor to the high dissolved inorganic carbon in the Yellow River. Chem Geol 430:34–44. doi:10.1016/j.chemgeo.2016.03.018

White AF, Blum AE (1995) Effects of climate on chemical_ weathering in watersheds. Geochim Cosmochim Acta 59:1729–1747

Wu L, Huh Y, Qin J, Du G, van Der Lee S (2005) Chemical weathering in the Upper Huang He (Yellow River) draining the eastern Qinghai-Tibet Plateau. Geochim Cosmochim Acta 69:5279–5294. doi:10.1016/j.gca.2005.07.001

Wu W (2016) Hydrochemistry of inland rivers in the north Tibetan Plateau: constraints and weathering rate estimation. Sci Total Environ 541:468–482. doi:10.1016/j.scitotenv.2015.09.056

Wu W, Xu S, Yang J, Yin H (2008) Silicate weathering and CO2 consumption deduced from the seven Chinese rivers originating in the Qinghai-Tibet Plateau. Chem Geol 249:307–320. doi:10.1016/j.chemgeo.2008.01.025

Xiao J, Jin ZD, Wang J, Zhang F (2015) Hydrochemical characteristics, controlling factors and solute sources of groundwater within the Tarim River Basin in the extreme arid region, NW Tibetan Plateau. Quaternary Int 380-381:237–246

Xiao J, Zhang F, Jin Z (2016) Spatial characteristics and controlling factors of chemical weathering of loess in the dry season in the middle Loess Plateau, China. Hydrol Process 30:4855–4869

Yoon J, Huh Y, Lee I, Moon S, Noh H, Qin J (2008) Weathering processes in the Min Jiang: major elements, $^{87}Sr/^{86}Sr$, $\delta^{34}SSO_4$ and $\delta^{18}OSO_4$. Aquat Geochem 14:147–170. doi:10.1007/s10498-008-9030-7

Zhong J, Li SL, Tao F, Yue F, Liu CQ (2017) Sensitivity of chemical weathering and dissolved carbon dynamics to hydrological conditions in a typical karst river. Sci Rep 7:42944. doi:10.1038/srep42944